

Compact Broadband Bandpass Filter on Quarter-Mode Substrate Integrated Waveguide Loaded with CRLH Interdigital Slots

Zhihua Wei, Jie Huang*, Yanhui Geng, Jing Li, and Guoqing Xu

Abstract—A compact broadband bandpass filter (BPF) on Composite right/left-handed (CRLH) Quarter-Mode Substrate Integrated Waveguide (QMSIW) is presented and analyzed in this paper. A size reduction is implemented by etching the CRLH interdigital slots (CRLH-IS) in the compact QMSIW cavity to introduce a lower resonant frequency less than that of the QMSIW. The influence of the rotation angle of the CRLH-IS on the frequency response of the CRLH QMSIW BPF is analyzed, and the optimal rotation angle is used to implement a BPF with good out-band rejection. The proposed CRLH QMSIW shows the characteristics of low quality factor and high coupling coefficient that make it a good solution to design a broadband bandpass filter. The measured insertion loss is less than 1.8 dB at 4.43 GHz with a fractional bandwidth (FBW) of around 22%. The measured results agree well with the simulated ones.

1. INTRODUCTION

With the rapid development of modern wireless communication systems, the demand for compact and high-performance microwave and millimeter wave bandpass filters has increased greatly over the last few decades. Special attention has been drawn to the substrate integrated waveguide (SIW) due to its high quality factor, low insertion loss, low cost, compact size and easy integration in the standard printed circuit board [1–4]. However, the SIW still suffers from large size for these applications at low frequency. A half-mode substrate integrated waveguide (HMSIW) has been proposed recently to reduce the size [5, 6]. To further realize the miniaturization, some resonators are loaded into the SIW or HMSIW, such as the CRLH-IS and complementary split ring [7–9]. However, high Q value and low coupling coefficient characterized by SIW and HMSIW cavities restrict their applications in the filed of broadband BPFs. Compared to the conventional SIW and HMSIW, the QMSIW has a much more compact size, lower quality factor and much stronger internal coupling coefficients of coupled cavities, and shows the great potential in compact broadband filter applications [10, 11].

In this paper, a compact broadband BPF based on QMSIW loaded by the CRLH-IS is proposed. A new resonant mode below the resonant frequency of the original dominant mode of the QMSIW cavity is introduced by etching the CRLH-IS in the QMSIW cavity, and the miniaturization of the proposed CRLH QMSIW cavity is achieved successfully. The low quality factor and strong coupling coefficient of QMSIW are used to design an ultra-wideband BPF with a broad FBW of 22%. And a good out-band rejection is implemented with the optimal rotation angle of the CRLH-IS. Compared to the conventional SIW [1], the BPF based on CRLH QMSIW offers a much broader bandwidth. To demonstrate the characteristics, the proposed BPF is fabricated and measured.

Received 4 March 2016, Accepted 24 March 2016, Scheduled 4 April 2016

* Corresponding author: Jie Huang (jiehuang@swu.edu.cn).

The authors are with the College of Engineering and Technology, Southwest University, Chongqing 400715, China.

2. ANALYSIS OF THE PROPOSED RESONATOR

The proposed CRLH QMSIW cavity, designed on a substrate RO4350 with a thickness of 10 mil and dielectric constant of $\epsilon_r = 3.66$, is shown in Fig. 1. The two neighboring arrays of metallized via-holes are used to create the metallic walls for the QMSIW cavity. The other two neighboring sides without metallized via-holes are open to the air and then some leakage of electromagnetic energy may happen.

The CRLH-IS must be placed with a rotation angle α on the top metal to meet its requirement for the propagation of electromagnetic wave in the CRLH QMSIW cavity. According to the layout of CRLH QMSIW resonators defined below in the filter, the simulation model is established to analyze the dependence of frequency response of CRLH QMSIW resonator on the rotation angle α , and is inserted in the Figs. 2(a) and (b), respectively. The corresponding simulated S_{21} and S_{11} at different rotation angles α are shown in Fig. 2. It is noticed that the QMSIW loaded by CRLH-IS has a dual-mode and dual resonance frequencies while the higher mode is undesired as it will cause the problem of spurious passband. The resonant frequency of the higher mode decreases and becomes close to that of the lower one as α increases. Especially, when α increases to 45° the two modes merge into one and operate at the same resonant frequency, and the merged resonant frequency of CRLH QMSIW is consistent with that of the Ref. [9] due to the same dimension of CRLH-IS. The spurious passband in the frequency response of the proposed BPF deteriorates the characteristics of out-band rejection, which will be confirmed in Section 3. So the rotation angle of 45° is used to design the high performance BPF with a good out-band rejection.

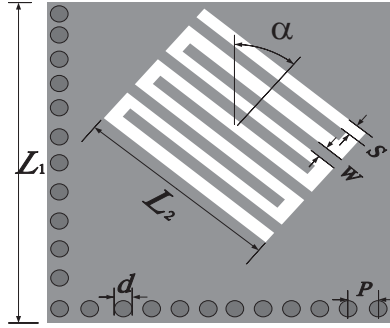


Figure 1. The layout of the proposed CRLH QMSIW cavity. The design parameters: $L_1 = 8$ mm, $L_2 = 5.4$ mm, $s = 0.2$ mm, $W = 0.2$ mm, $d = 0.4$ mm, $p = 0.5$ mm, $\alpha = 45^\circ$.

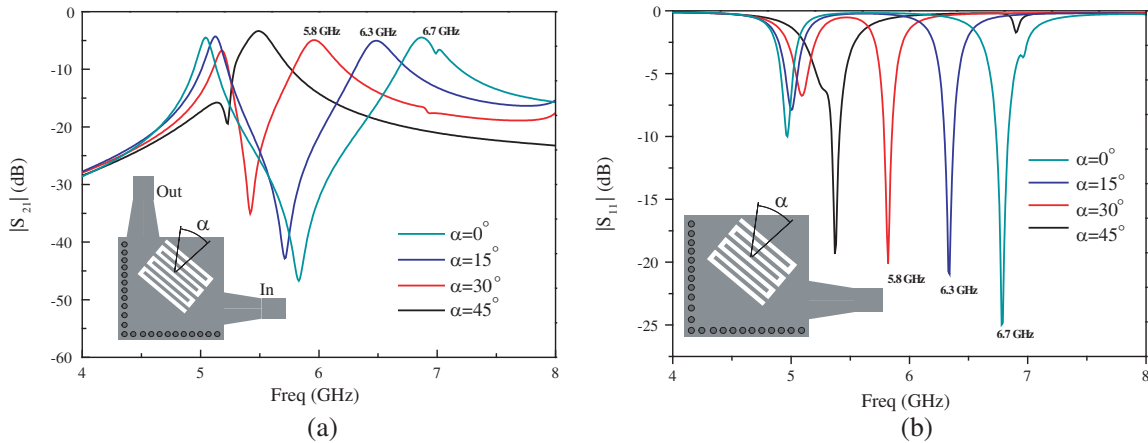


Figure 2. (a) The simulated $|S_{21}|$ of a single doubly-loaded QMSIW CRLH cavity with different rotation angles α . (b) The simulated $|S_{11}|$ of a single QMSIW CRLH cavity with different rotation angles α .

Figure 3 illustrates the magnitude of the electric field distribution for a conventional SIW cavity at 7 GHz, the original QMSIW cavity at 7 GHz and the proposed CRLH QMSIW cavity at 5 GHz. The simulations are performed by Ansoft HFSS. Fig. 3(a) indicates that the maximum E -field of the dominant TE_{101} mode locates at the center of the conventional square SIW cavity, so the symmetrical planes AA' and BB' can be regarded as two equivalent magnetic walls. And then the QMSIW cavity is generated by bisecting the SIW with the two fictitious magnetic walls. As shown in Fig. 3(b), the maximum E -field of the dominant TE_{101} mode locates at the corner of the QMSIW cavity, and the QMSIW cavity propagates one-quarter of the quasi- TE_{101} mode in the original SIW cavity. The QMSIW cavity represents one-quarter of the SIW cavity, and has a 75% size reduction with the same resonant frequency. However, the resonant frequency of the QMSIW cavity will be a little lower than that of the original SIW cavity because the two open edges of QMSIW cavity are not perfect magnetic walls and some leakage of electromagnetic energy may happen.

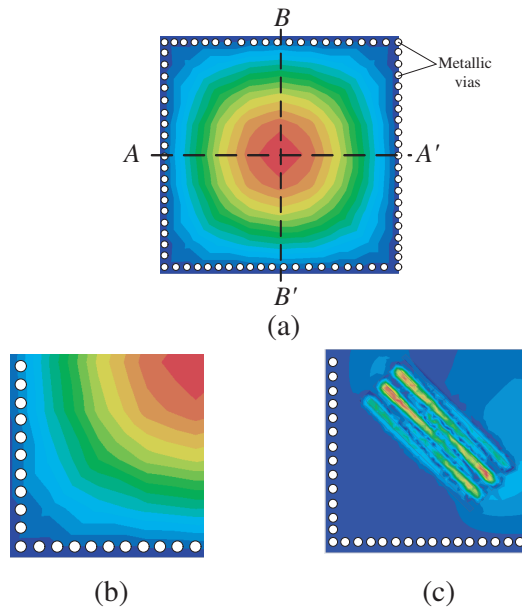


Figure 3. The magnitude of the electric field distributions in various cavities. (a) TE_{101} mode E -field in the SIW cavity at 7 GHz. (b) One-quarter of the quasi- TE_{101} mode E -field in the QMSIW cavity at 7 GHz. (c) E -field in the CRLH QMSIW cavity at 5 GHz.

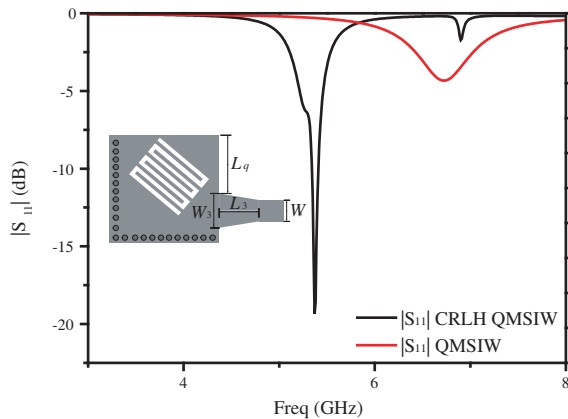


Figure 4. Frequency responses of the CRLH QMSIW cavity and the original QMSIW cavity.

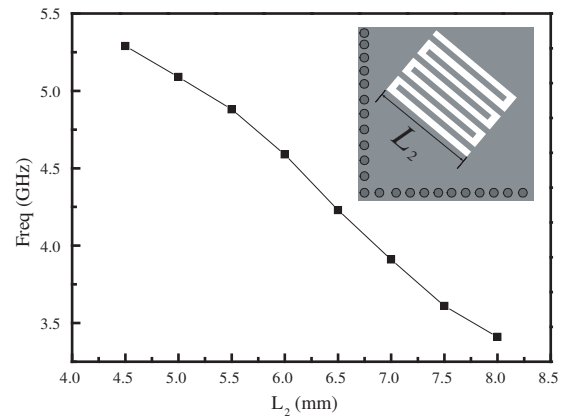


Figure 5. The resonant frequency of the CRLH QMSIW cavity with different lengths of the CRLH-IS L_2 .

The CRLH is loaded into the QMSIW cavity to introduce a much lower resonant frequency and further reduce the size. One tapered-feedline is used to excite the cavity. Fig. 4 shows the comparison of the simulated frequency response between the QMSIW cavity and the CRLH QMSIW cavity with the same size. It can be observed that the main mode of the cavity decreases from 6.8 GHz to 5.2 GHz when the CRLH-IS is loaded on, and the CRLH QMSIW cavity propagates a new resonant mode below the resonant frequency of the QMSIW cavity.

Figure 5 shows the dependence of the resonant frequency of the CRLH QMSIW cavity on the length of the CRLH-IS L_2 . It can be found that the resonant frequency tends to drop as L_2 increases. It means that the resonant frequency can be controlled by the length of the CRLH-IS with the overall size of the cavity unchanged.

3. FILTER DESIGN

A four-pole Chebychev BPF with a center frequency of 4.5 GHz and a FBW of 22% is designed to demonstrate the design concept. Fig. 6(a) depicts the configuration of the four-pole Chebychev BPF based on the CRLH QMSIW cavity. The corresponding coupling scheme is presented in Fig. 6(b). With the circuit elements of the low-pass prototype filter, these filter parameters, namely the external quality factor of Q and coupling coefficient of K , can be determined by the classical design procedure of BPFs in [12], and is shown in Eq. (1), where FBW is the fraction bandwidth.

$$Q_e = \frac{g_1}{FBW}, \quad k_{12} = k_{34} = \frac{FBW}{\sqrt{g_1 g_2}}, \quad k_{23} = \frac{FBW}{\sqrt{g_2 g_3}} \quad (1)$$

Following the design procedure, the coupling coefficients of the BPF are $K_{12} = K_{34} = 0.215$, $K_{23} = 0.166$, and the Q value is 3.99. A single cavity with one tapered-feedline and two coupled cavities are simulated to obtain these values of K and Q , respectively. The relationship between the coupling coefficient K and the window width W_c is shown in Fig. 7(a), and indicates that the coupling coefficient K is controlled by the window width W_c between two cavities. Based on the required coupling coefficients given above, the window widths can be extracted from the plot in Fig. 7(a). And the quality factor Q is determined by the offset distance L_q from the feedline to the open corner. Then the distance L_q can also be obtained from the relationship plot in Fig. 7(b). As shown in Fig. 7, the CRLH QMSIW cavity shows a low external quality factor Q . At the same time, a much stronger coupling coefficient, which can be hardly obtained in the conventional SIW, is achieved with a proper value of W_c . As observed from the Eq. (1), a broad bandwidth requires a low Q value and high coupling coefficients. Therefore, the CRLH QMSIW cavity can be used to design broadband BPFs.

To further verify the influence of the rotation angle α on the frequency response of the proposed BPF mentioned in Section 2, four BPFs with the layout shown in Fig. 6(a) with $\alpha = 0^\circ, 15^\circ, 30^\circ, 45^\circ$ are simulated, respectively. The corresponding frequency response is shown in Fig. 8, where the

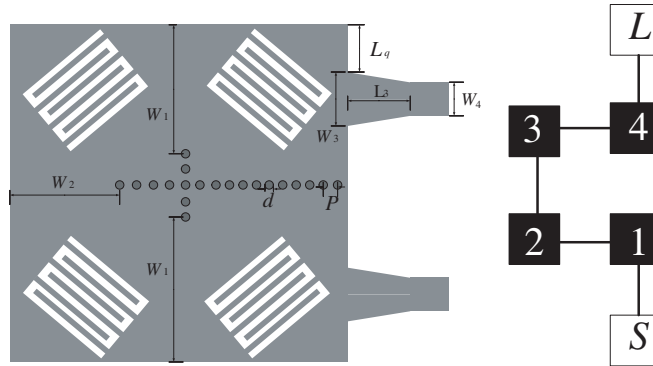


Figure 6. (a) The configuration of the CRLH QMSIW BPF. The physical dimensions: $L_q = 0$ mm, $W_1 = 6.5$ mm, $W_2 = 3.77$ mm, $d = 0.4$ mm, $p = 0.5$ mm, $W_3 = 4$ mm, $L_3 = 3$ mm, $W_4 = 0.53$ mm. (b) The coupling scheme of the CRLH QMSIW BPF.

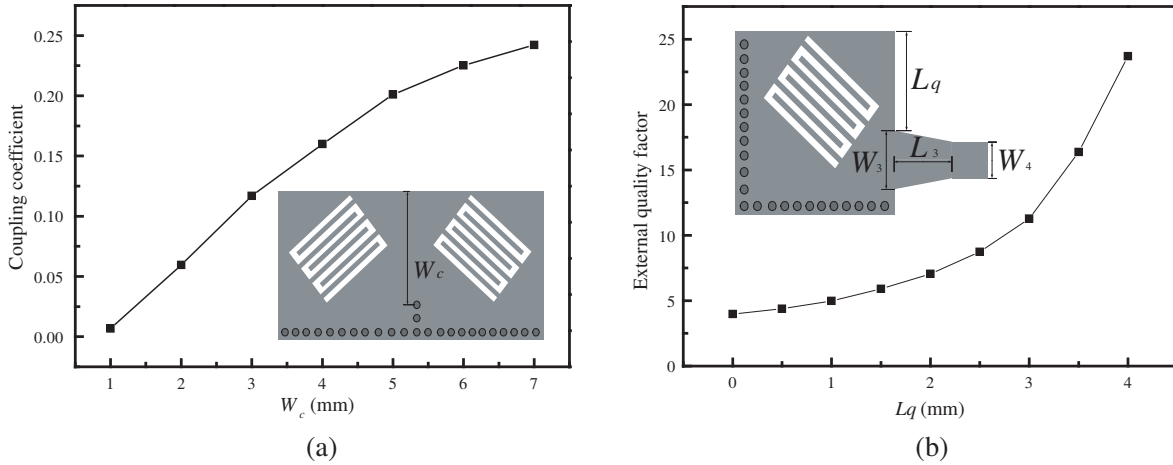


Figure 7. Coupling coefficient between the CRLH QMSIW cavities and the external quality factor of the CRLH QMSIW cavity. (a) Coupling coefficient versus window width W_c . (b) External quality factor versus L_q , the physical dimensions: $W_3 = 4$ mm, $L_3 = 3$ mm, $W_4 = 0.53$ mm.

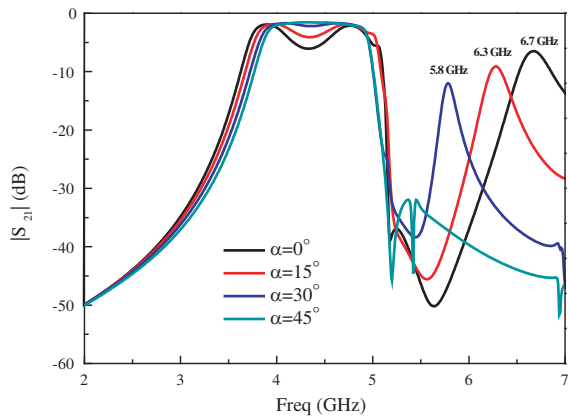


Figure 8. The simulated $|S_{21}|$ of the four BPFs with different rotation angles α .

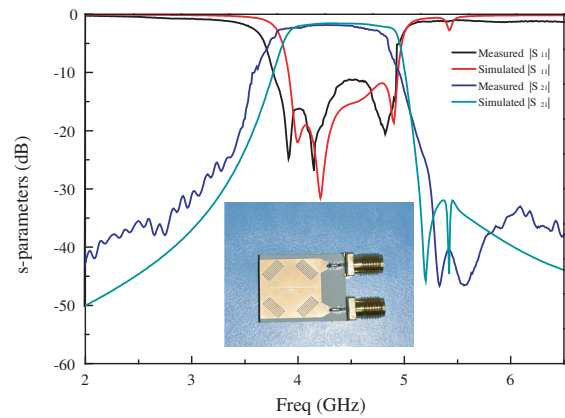


Figure 9. Simulated and measured results of the CRLH QMSIW BPF.

problem that the spurious passband in the frequency response of the proposed BPF deteriorates the characteristics of out-band rejection can be confirmed. It is noticed that there are three spurious passbands located at 5.8, 6.3 and 6.7 GHz at $\alpha = 0^\circ, 15^\circ, 30^\circ$, respectively. And these frequencies of the spurious passbands are consistent with that of the higher modes shown in Fig. 2. When α increases to 45° , the spurious passband disappears due to the fact that the two modes of the CRLH QMSIW cavity have merged into one and operate at the same resonant frequency, resulting in a good out-band rejection. And then the optimal rotation angle of 45° is applied to implement the compact broadband BPF with good out-band rejection.

4. SIMULATED AND MEASURED RESULTS

Based on above analysis and simulation, the CRLH QMSIW BPF was fabricated and measured. The measurements were performed with a network analyzer (Agilent E5071C). The measured results are compared with the simulated ones in Fig. 9, and a good agreement between them is achieved except a frequency shift of around 1.5%. The frequency shift is partly caused by the tolerances of the fabrication and the metallization procedures. The measured central frequency locates at 4.43 GHz, and a 3-dB FBW of around 22% is achieved. The minimum insertion loss is less than 1.8 dB, and is mainly from

the losses of the conductor, dielectric and the SMA connectors. The in-band return loss is better than 11 dB. A steep cutoff frequency at the right edge of the passband is implemented with two transmission zeros introduced by the CRLH-IS.

The measured broadband BPF performance is compared with other high performance QMSIW BPFs, as shown in Table 1. Compared with BPFs reported in [10], the proposed one has a smaller size. And the proposed BPF offers a much broader FBW than BPFs in [13] and [14].

Table 1. Comparison between the proposed filter and previous works.

Reference	Size	FBW
[10]-1	$0.56\lambda_g * 0.56\lambda_g$	14%
[10]-2	$0.52\lambda_g * 0.51\lambda_g$	26%
[13]	$0.25\lambda_g * 0.25\lambda_g$	11.6%
[14]-1	$0.16\lambda_g * 0.15\lambda_g$	9.8%
This work	$0.39\lambda_g * 0.39\lambda_g$	22%

* λ_g is the guide wavelength at the central frequency.

5. CONCLUSION

In this paper, a compact ultra-broadband CRLH QMSIW BPF is designed, fabricated and measured. A FBW of around 22% is achieved successfully due to the low quality factor and high internal coupling coefficient of the CRLH QMSIW cavity. The compact CRLH-IS and miniaturized QMSIW cavity are combined to implement an ultra-compact BPF with a more than 75% size reduction. And the out-band rejection of the BPF is improved by optimizing the rotation angle of the CRLH-IS. The broad FBW, good out-band rejection and compact size make the proposed CRLH QMSIW BPF more competitive for microwave applications.

ACKNOWLEDGMENT

This work was supported by the Young Scientists Fund of the National Natural Science Foundation, China (Grant No. 61401373) and by the Research Fund for the Doctoral Program of Southwest University, China (Grant No. SWU111030).

REFERENCES

1. Chen, X., W. Hong, T. Cui, J. Chen, and K. Wu, "Substrate integrated waveguide (SIW) linear phase filter," *IEEE Microwave and Wireless Components Letters*, Vol. 15, 787–789, Nov. 2005.
2. Deslandes, D. and K. Wu, "Single-substrate integration technique of planar circuits and waveguide filters," *IEEE Trans. Microwave Theory Tech.*, Vol. 51, 593–596, Feb. 2003.
3. Cassivi, Y., L. Perregrini, P. Arcioni, M. Bressan, K. Wu, and G. Conciauro, "Dispersion characteristics of substrate integrated rectangular waveguide," *IEEE Microwave and Wireless Components Letters*, Vol. 12, 333–335, 2002.
4. Deslandes, D. and K. Wu, "Integrated microstrip and rectangular waveguide in planar form," *IEEE Microwave and Wireless Components Letters*, Vol. 11, 68–70, 2001.
5. Wang, Y., W. Hong, Y. Dong, B. Liu, H. J. Tang, J. Chen, X. Yin and K. Wu, "Half mode substrate integrated waveguide (HMSIW) bandpass filter," *IEEE Microwave and Wireless Components Letters*, Vol. 17, No. 4, 265–267, Apr. 2007.
6. Liu, B., W. Hong, Y.-Q. Wang, Q.-H. Lai, and K. Wu, "Half mode substrate integrated waveguide (HMSIW) 3-dB coupler," *IEEE Microwave and Wireless Components Letters*, Vol. 17, 22–24, Jan. 2007.

7. Dong, Y. and T. Itoh, "Composite right/left-handed substrate integrated waveguide and half-mode substrate integrated waveguide," *IEEE MTT-S Int. Microw. Symp. Dig.*, 49–52, Boston, 2009.
8. Dong, Y. and T. Itoh, "Promising future of metamaterials," *IEEE Microwave Magazine*, Vol. 13, No. 2, 39–56, Mar.–Apr. 2012.
9. Zhao, Q., Z. L. Chen, J. Huang, G. Li, Z. Zhang, and W. Dang, "Compact dual-band bandpass filter based on composite right/left-handed substrate integrated waveguide loaded by complementary split-ring resonators defected ground structure," *Journal of Electromagnetic Waves and Applications*, Vol. 28, No. 14, 1807–1814, 2014.
10. Zhang, Z., N. Yang, and K. Wu, "5-GHz bandpass filter demonstration using quarter-mode substrate integrated waveguide cavity for wireless systems," *Proceedings of IEEE Radio and Wireless Symposium*, 95–98, 2009.
11. Zhang, S, T. Bian, Y. Zhai, W. Liu, G. Yang, and F. Liu, "Quarter substrate integrated waveguide resonator applied to fractal-shaped BPFs," *Microw. Journal*, Vol. 55, No. 5, 200–208, May 2012.
12. Mattaei, G. L., L. Young, and E. M. T. Tones, *Microwave Filters, Impedance-Matching Network, and Coupling Structures*, Artech House, Norwood, MA, 1980.
13. Senior, D. E., A. Rahimi, and Y.-K. Yoon, "A surface micromachined broadband millimeter-wave filter using quarter-mode substrate integrated waveguide loaded with complementary split ring resonator," *2014 IEEE MTT-S Int. Microwave Symp. Dig.*, 1-4, Jun. 2014.
14. Huang, Y., Z. Shao, C. You, and G. Wang, "Size-reduced bandpass filters using quarter-mode substrate integrated waveguide loaded with different defected ground structure patterns," *2015 IEEE MTT-S Int. Microwave Symp. Dig.*, 1–4, 2015.